Supplement

M. Schwaerzel et al.

S1 Additional information

S1.1 Example of a MYSTIC NetCDF input file for the urban canopy

```
netcdf triangle_example {
    dimensions:
            Nvert = 6 ;
            Ndim = 3 ;
            Ntriangles = 5 ;
            Ncorner = 3 ;
            N_materials = 4 ;

    variables:
            double vertices(Nvert, Ndim) ;
                    vertices:_FillValue = NaN ;
            int64 triangles(Ntriangles, Ncorner) ;
            int64 material_of_triangle(Ntriangles) ;
            double material_albedo(N_materials) ;
                    material_albedo:_FillValue = NaN ;
            string material_type(N_materials) ;
            double temperature_of_triangle(Ntriangles) ;
                    temperature_of_triangle:_FillValue = NaN ;
    data:

     vertices =
            5.56999999994878, -6.07999999998719, 8.2,
            5.56999999994878, -6.07999999998719, 0,
            -3.09999999997672, 4.48000000001048, 8.2,
            -3.09999999997672, 4.48000000001048, 0,
```

```
                6.40000000002328, 12.320000000007, 8.2,
                6.40000000002328, 12.320000000007, 0;

        triangles =
                0, 2, 5,
                0, 2, 1,
                1, 2, 3,
                2, 4, 5,
                2, 4, 3,

        material_of_triangle = 0, 1, 1, 0, 1;

        material_albedo = 0.1, 0.1;

        material_type = "roof", "wall";

        temperature_of_triangle = 273.15, 273.15, 273.15, 273.15, 273.15;
}
```

The MYSTIC NetCDF input file for the urban canopy contains a temperature for each triangle, which is not used in the radiative transfer calculations for this study, but needs to be set for avoiding a error message from the MYSTIC model.

S1.2 MYSTIC inputs

Table S1. MYSTIC inputs for AMFs simulations.

Parameter	Value
Number of photons	50000 or 500000
Wavelength [nm]	490
Solar zenith angle [°]	60 or 30
Solar azimuth angle [°]	0, 90
Viewing zenith angle [°]	0.24 - 5.47
Viewing azimuth angle [°]	90, 270
Surface albedo	0.1 or 0.2
Aircraft position x [m]	600
Aircraft position y [m]	2.5 - 997.5
Aircraft position z [m]	6000
Simulation domain [boxes]	20×20×41
Horizontal resolution [m]	5 or 50
Vertical resolution (0 - 45m) [m]	5
Vertical resolution (50 - 1000m) [m]	100
Vertical resolution (1000 - 1500m) [m]	250
Vertical resolution (2000 - 21000m) [m]	1000
Aerosol absorption and scattering	off

S1.3 3D NO_2 concentration field

To obtain a realistic synthetic 3D NO_2 concentration field, we proceeded as following:

- We summed emissions from cars, busses, trucks and motorbikes from the 2015 road emission inventories from the city of Zurich.
- We rasterized the emission field to a 5 m x 5 m resolution grid and divided each grid cell by the maximum grid cell value.
- We multiplied the obtained 2D field with a concentration of 110 [$\mu g\ m^{-3}$] and added a background of 15 [$\mu g\ m^{-3}$], which are respectively typical high and background values found at measurement stations close

to the road and on a background site (e.g. https://www.stadt-zuerich.ch/gud/de/index/umwelt_energie/luftqualitaet/messdaten/verlauf-24-stunden.html, last access: 26 July 2021). Finally, we smoothed the concentration field with a Gaussian filter with a standard deviation of 5 m to mimic the effect of turbulent dispersion.

- From the obtained ground concentration map we created 3D concentrations applying the following function to every ground pixel. Between $h_0 = 0$ m and $h_1 = 100$ m a linear concentration decrease with altitude was applied with the level corresponding concentrations c_0 = ground concentration (grid cell concentration) and c_1 = 1/5 of the ground concentration over a background pixel. From h_1 upwards, an exponential decay function (A exp(t z) + y0) with A = 1.6, t = -1.39 and y0 = 0.09 parameters was applied. These parameters were defined by fitting a function to a measured NO_2 profile from the MuNIC campaign.

- Finally the VCD calculated using the created 3D NO_2 concentration field was compared with NO_2 VCDs from the MuNIC measurement campaign (2016).

S2 Additional figures

S2.1 SCDs for a solar zenith angle of 30°

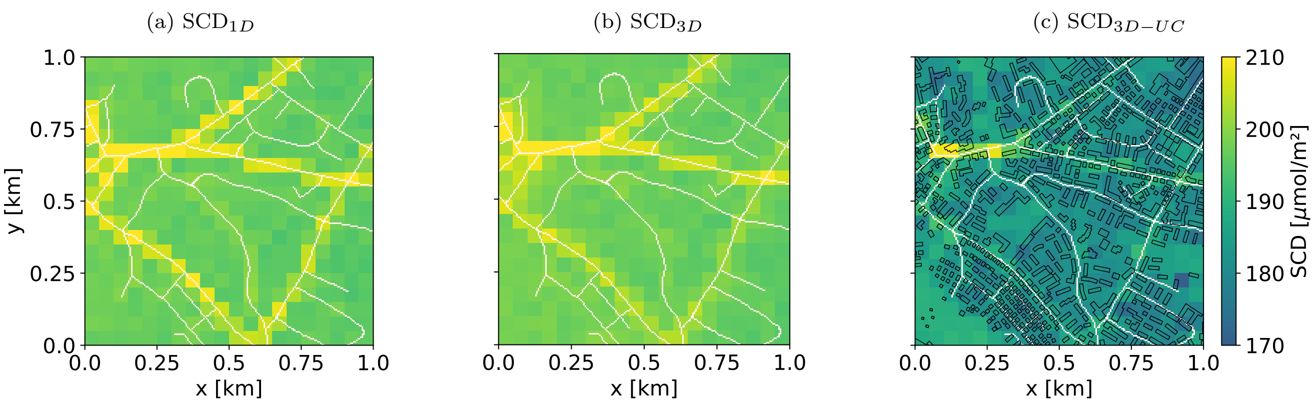

Figure S1. SCDs for a simulation with SZA of 30° with (a) 1D-layer AMFs simulation, 3D-box AMFs (b) without and (c) with buildings. The roads are drawn in white and the building contours in black for the simulation with buildings.

S2.2 SCDs difference plot for a solar zenith angle of 30°

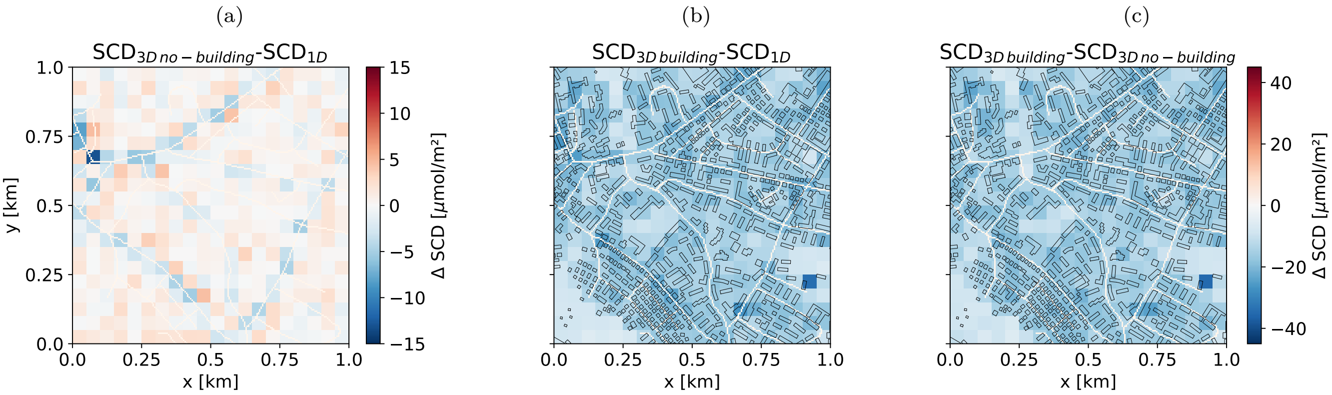

Figure S2. Difference plots for SCDs calculated with a solar zenith angle of 30°. (a) Difference plot between SCDs calculates with 3D-box AMFs and the SCDs calculated with 1D-layer AMFs. (b) Difference plot between SCDs calculated with 3D-box AMFs including buildings and SCDs calculated with 1D-layer AMFs. (c) Difference plot between SCDs calculated with 3D-box AMFs with and without buildings.

S2.3 Increased roof albedo for the high resolution scenario

Here we show the impact of an increased albedo on the building roofs. We changed the albedo of the roofs from 0.1 to 0.2.

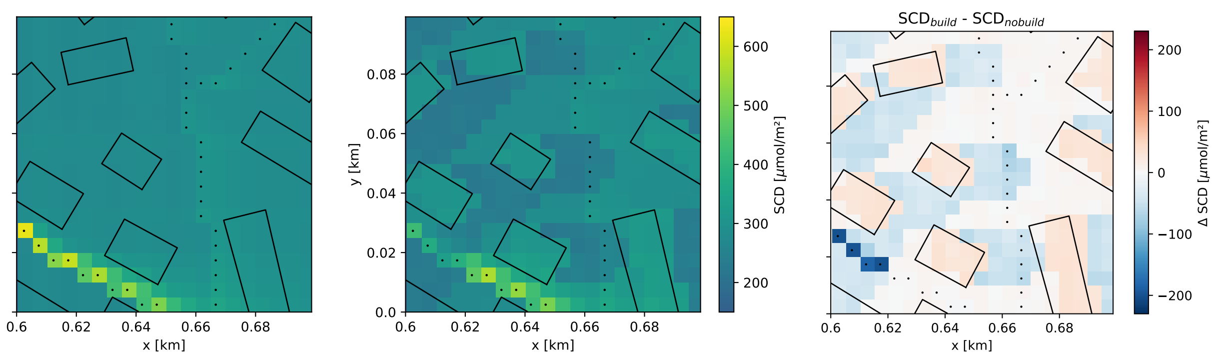

Figure S3. SCDs for a SAA of 90° for 3D-box AMFs simulation (a) without and (b) with buildings and (c) the difference between both. The roof albedo was changed to 0.2. The roads are drawn with dots and the building contours in black

We observe the increase in AMFs and therefore SCDs above the buildings because more photons are scattered on the roof with a higher albedo, compared to the lower ground albedo.

S2.4 SCDs for a solar azimuth angle of 270°

We also computed SCDs with the 3D-box AMFs module for a SAA=270° (see Figure S4). Similarly to observations made in the main text, SCD are smeared mostly in the direction of the main optical path (E-W-direction).

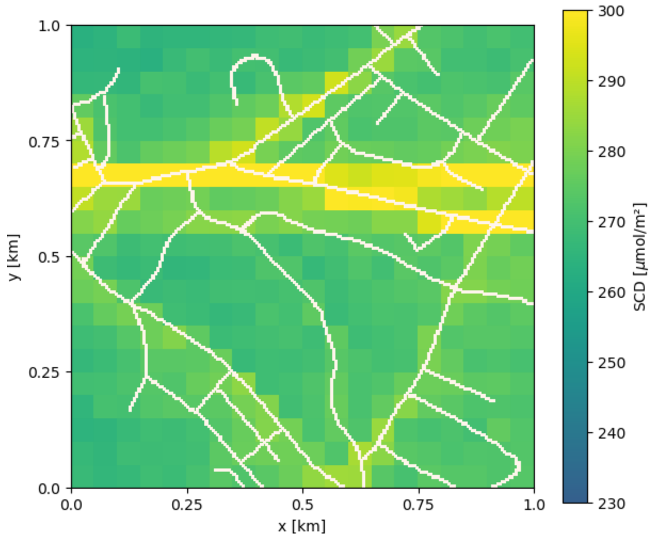

Figure S4. SCD without buildings and a SAA of 270°

S2.5 SCDs for simulations at 420 nm

We also computed SCDs with the 1D-layer and 3D-box AMFs module at a wavelength of 420 nm. The mean value of the field is decreased by approximately 12% for the 1D and 3D simulations with and without buildings compared to simulations at 490 nm.

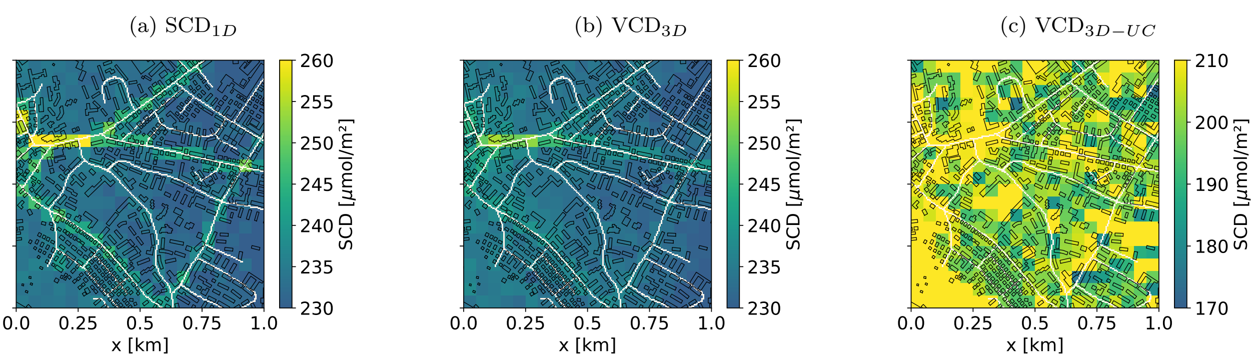

Figure S5. SCD from (a) 1D-layer AMFs and 3D-box (b) without and (c) with buildings at 420 nm

S2.6 Retrieving VCDs from SCDs

Figure S6 shows VCDs retrieved from the assumed "true" SCD_{3D} using (a) 1D-layer AMFs and (b) 3D-box AMFs. Here 1D-layer AMFs used to retrieve VCDs fails to correct for the spatially smeared SCD field.

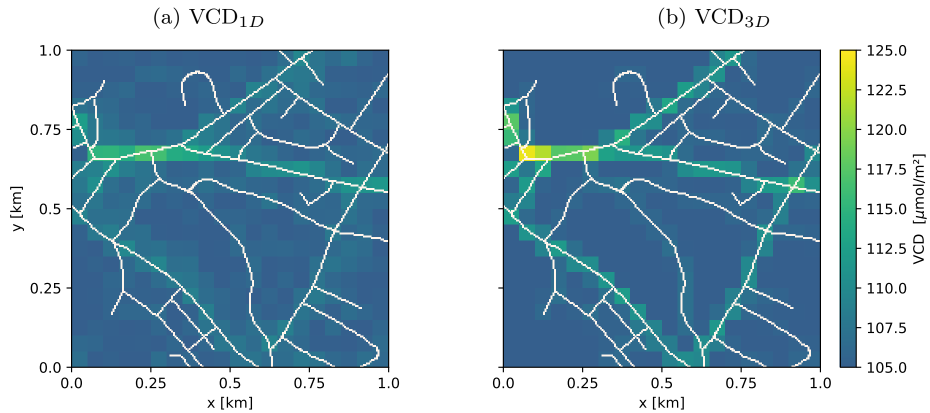

Figure S6. VCDs retrieved with (a) 1D-layer AMFs and (b) 3D-box AMFs without buildings.

S2.7 Footprints

S2.7.1 Footprints with aerosols

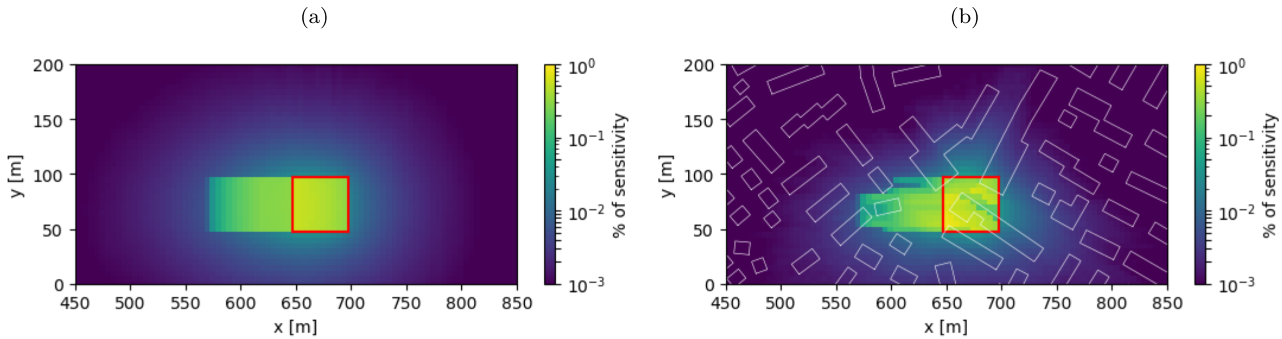

Figure S7. (a) Footprint without buildings and with aerosols. 55.2% of the signal is located outside the ground pixel (i.e. outside the red frame). (b) Footprint with buildings and aerosols. 55.2% of the instrument sensitivity is located outside the ground pixel. Building contours are drawn in white.

S2.7.2 Footprints for a solar zenith angle of 20° and 40°

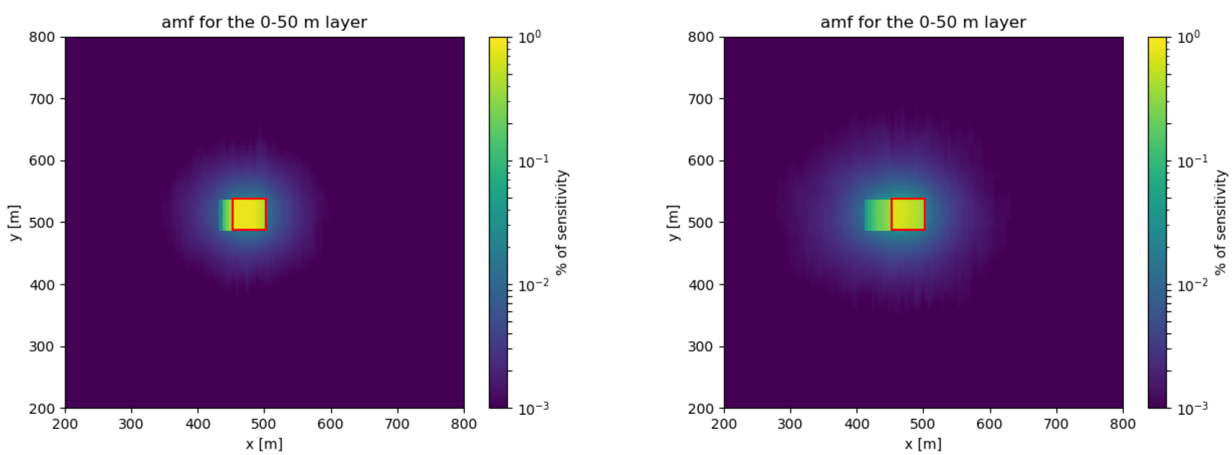

Figure S8. Effect of SZA on APEX footprint. Simulation with SZA = 20° and 40°. Respectively 27.4% and 45.2% of the sensitivity is located outside the ground pixel (red square).

S3 Computational time

S3.1 Simulations with buildings

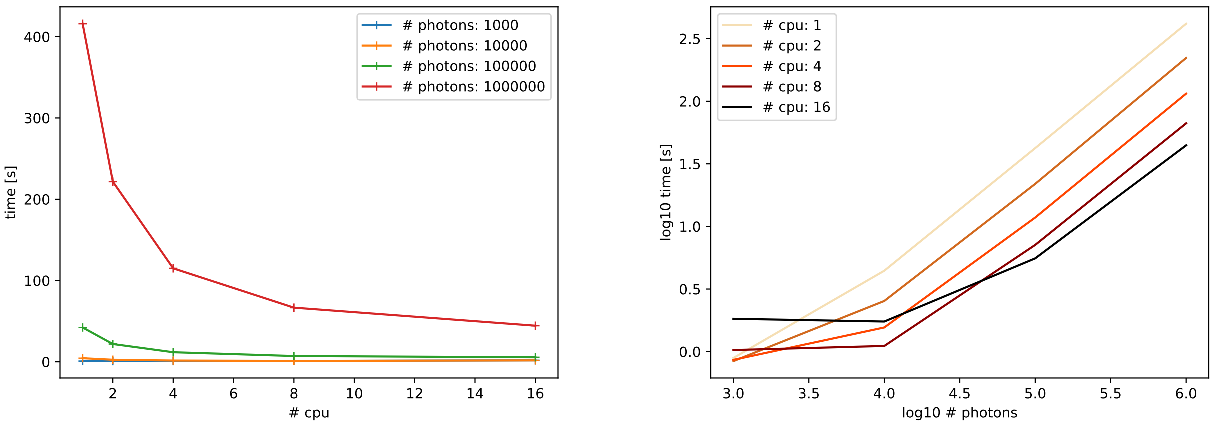

Figure S9. Computational time for simulations with buildings depending on (left) amount of used CPUs and (right) amount of photons used for a single simulation.

S3.2 Simulations without buildings

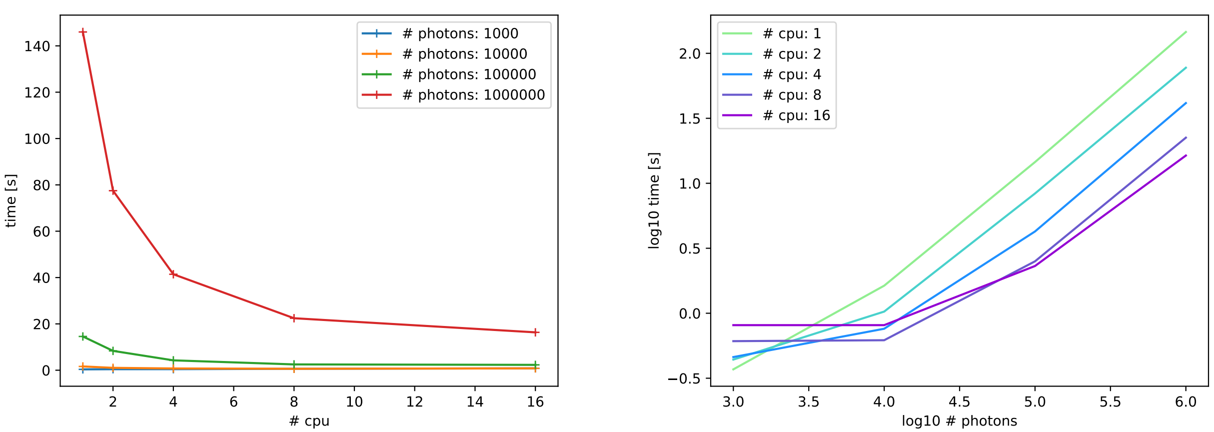

Figure S10. Computational time for simulations without buildings depending on (left) amount of CPUs used and (right) photon amount used for a single simulation.